Pore Creation in Silicon Oxycarbides by Rinsing in Dilute Hydrofluoric Acid

A. M. Wilson,† G. Zank,‡ K. Eguchi,‡ W. Xing,§ B. Yates,⊥ and J. R. Dahn*,§

Department of Physics, Simon Fraser University, Burnaby, BC, Canada V5A 1S6; Dow Corning Asia Ltd., Yamakita, Kanagawa, Japan; Departments of Physics and Chemistry, Dalhousie University, Halifax, NS, Canada B3H 3J5; and Canadian Synchrotron Radiation Facility, University of Western Ontario, London, Ontario, Canada

Received April 16, 1997. Revised Manuscript Received July 10, 1997⊗

We have prepared silicon oxycarbides by the pyrolysis of siloxane polymers at a maximum temperature of 1000 °C. The resulting silicon oxycarbides are networked glasses which we believe also contain some graphene sheets. After washing in a dilute solution of hydrofluoric acid for times between 2 min and 24 h, these materials lost, at most, 40% of their mass. Powder X-ray diffraction (XRD), small-angle scattering (SAX), BET surface area measurements, elemental analysis, and silicon K-edge X-ray absorption spectroscopy (XAS) were used to determine the physical structure of the bulk material and the local chemical environments of the Si atoms. It was found that a microscopic pore network was created in the material upon HF washing. The number of pores, but not their size, increased with HF washing time. The HF etching revealed a passivating layer, which we believe consists mainly of silicon and carbon, that prevented further etching of the material. The electrochemical behavior of these materials in Li batteries was not affected by the radical changes in surface chemistry.

Introduction

Silicon polymers are commonly used in the production of silicon carbide and silicon oxycarbides.[1,2] We have experience in the pyrolysis of siloxane polymers for use in Li-ion cells.[3−6] Depending on the material desired, one chooses appropriate polymers and pyrolysis parameters. Typically, silicon carbide will be produced upon pyrolysis at sufficiently high temperatures.[1−3] We showed previously[6] that the Si−O−C glasses with the highest reversible capacities for lithium (about 900 mAh/g) were found at a composition of about 43% (atomic) carbon, 32% oxygen, and 25% silicon. However, these materials had large irreversible capacities[6] as well. In ref 6, it was shown that the magnitude of the irreversible capacity increased with the oxygen content of the material. Since HF is known to dissolve SiO_2, we hoped that the oxygen content of these materials could be reduced, and consequently the electrochemical properties improved, by a room-temperature HF treatment of the Si−O−C glasses.

Here, we started with a common highly cross-linked polysiloxane, and then pyrolyzed it at a temperature sufficiently high to ensure complete decomposition of the polymer to a silicon oxycarbide glass (Si−O−C), but low enough that the oxygen was not driven out of the material, forming silicon carbide. The resulting material was washed in dilute hydrofluoric acid, and the properties of the washed samples were studied. In addition to removing oxygen, the HF also removed silicon and some carbon, leading to a small increase in the percentage of carbon in the material. Up to 40% of the initial sample mass could be dissolved, and then, surprisingly, dissolution stopped. Micropores having a characteristic size of about 1 nm were created by the HF etching, but these did not grow larger with etching time. Their number, however, did increase with etching time. The electrochemical behavior of the samples did not change, despite the changes to their physical properties and stoichiometry. Here we describe these experiments carefully and present a model to explain these surprising results.

Experiment

The polysiloxane precursor was synthesized as explained elsewhere.[6,7] The resulting polymer had a stoichiometry of $[ViSiO_{1.5}]_{0.66}[MeSiO_{1.5}]_{0.09}[Me_2ViSiO_{0.5}]_{0.25}$. Here, Vi and Me designate vinyl and methyl groups, respectively. The polysiloxane was held in a graphite crucible and heated under constant argon purge in a Lindberg Model 54434 furnace. The argon flush rate was sufficient to prevent the decomposition and redeposition of vapors released during polymer decomposition. The temperature was raised at a rate of 5 °C/min to 1000 °C and held for 1 h. Cooling to 100 °C was at a rate of approximately 3−4 °C/min. The reaction tube was then

* To whom correspondence should be addressed.
† Simon Fraser University.
‡ Dow Corning Asia Ltd.
§ Dalhousie University.
⊥ University of Western Ontario.
⊗ Abstract published in *Advance ACS Abstracts,* September 15, 1997.
(1) Burns, G. T.; Taylor, R. B.; Xu, Y.; Zangvil, A.; Zank, G. A. *Chem. Mater.* **1992**, *4*, 1313−1323.
(2) Abu-eid, M. A.; King, R. B.; Kotliar, A. M. *Eur. Polym. J.* **1992**, *28*, 315−320.
(3) Wilson, A. M.; Reimers, J. N.; Fuller, E. W.; Dahn, J. R. *Solid State Ionics* **1994**, *74*, 249−254.
(4) Wilson, A. M.; Zank, G.; Eguchi, K.; Xing, W.; Dahn, J. R. Paper I−A-8 presented at the 8th International Meeting on Lithium Batteries, Nagoya, Japan June 16−21, 1996, also accepted for publication in *J. Power Sources*.
(5) Xing, W.; Wilson, A. M.; Zank, G.; Dahn, J. R. *Solid State Ionics*, in press.
(6) Xing, W.; Wilson, A. M.; Zank, G.; Eguchi, K.; Dahn, J. R. *J. Electrochem. Soc.*, submitted.
(7) Dahn, J. R.; Wilson, A. M.; Xing, W.; Zank, G. A. Electrodes for Li-ion Batteries Using Polysiloxanes. U.S. Patent Application 664278, June 1996.

S0897-4756(97)00224-X CCC: $14.00

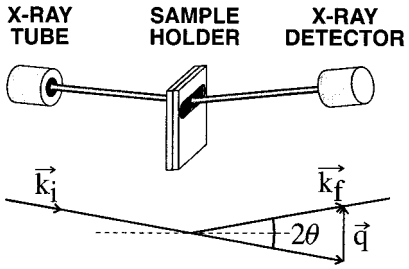

Figure 1. (a) Small-angle scattering apparatus and (b)-schematic showing k_i, k_f, and q.

removed from the furnace and allowed to cool to ambient room temperature before opening to the air. The material reclaimed was ground to a powder by a rolling ball grinder.

Sample 1 was prepared by rinsing a portion of the ground Si−O−C sample in distilled water. Samples 2−9 were prepared by washing portions of the ground Si−O−C sample in an HF solution. HF washing was performed by immersing the powders in a solution of HF (20 vol % in H_2O) in stoichiometric excess to the oxygen present in the initial Si−O−C. After stirring the resulting slurry for a specific period of time, varying from 15 min to 24 h, the sample was recovered by filtering and rinsed with distilled water to remove any residual HF.

A Siemens D5000 powder X-ray diffractometer, equipped with a Cu target X-ray tube and a diffracted beam monochromator was used to characterize all the samples. The Bragg−Brentano (flat plate sample) geometry was used. Samples were prepared by filling a 25 mm × 16 mm × 2 mm deep well in a stainless steel plate with the powdered sample followed by a smoothing of the surface.

Small-angle X-ray scattering is measured by transmission in the same Siemens D5000 powder X-ray diffractometer operating in transmission mode, as shown in Figure 1. Powdered samples (50−100 μm thick) were held in a rectangular frame with Kapton windows (25 μm thick) on both sides. Data were collected between scattering angles of 0.3° and 15°. The scattering from the Kapton windows in this range is very small compared to that from the samples and can be neglected. We used 0.1° incident and antiscatter slits and a 0.1 mm receiving slit. The mass of the sample in the frame was recorded. The attenuation of the X-ray beam by the sample was measured by comparing the beam intensity (as detector counts per second) with and without the sample in the beam path while the tube and detector were set to 0°. The holder, either empty or filled with sample, was placed in the beam path.

The surface area of the materials was measured by the Brunauer−Emmett−Teller (BET) method. Single-point measurements were made using a Micrometrics Flowsorb surface area analyzer. A mixture of nitrogen in helium (30:70 mol. %) was used. The samples were degassed in this gas mixture at 140 °C for 10−15 min. The final results were taken from the desorption data.

The decomposition process of the polysiloxane was studied using a TA Instruments Model 951 thermal gravimetric analyzer (TGA) connected to a Leybold Quadrex 200 residual gas analyzer (RGA), as described elsewhere.[5]

Elemental analyses of all the materials discussed was performed by employees of Dow Corning Corp. (Midland, MI). CHN analysis were done using a Perkin-Elmer 2400 analyzer. Oxygen analyses were made on a Leco oxygen analyzer (model R0-316) equipped with an oxygen determinator 316 (Model 783700) and an electrode furnace EF100. Silicon analysis was determined by a fusion technique that consisted of converting the solid to a soluble form and analyzing the solute for total silicon by Arl 3580 ICP-AES analysis.

X-ray absorption measurements were performed at the Canadian Synchrotron Radiation Facility double-crystal monochromator beam-line, located at the Synchrotron Radiation Facility in Stoughton, WI. The operational details of the double-crystal monochromator have been explained elsewhere.[8] Figure 2 shows a schematic of the apparatus used. Samples under a vacuum not exceeding 1×10^{-6} Torr were exposed to monochromatic synchrotron radiation. The electrons excited from the material were collected by a loop of wire biased at 136 V located in front of the sample. To maintain electrical neutrality, a current, I_s, flows to the sample through a Keithley 427 current/voltage converter. The value of the sample current, I_S, is proportional to the total electron yield. The absorption measurements were made by measuring I_S, as a function of photon energy. A 1 Torr nitrogen gas cell is used to measure the beam strength which reaches the sample, I_0. The final Si K-edge signal is determined by dividing the I_S by I_0 and is hereafter referred to as the X-ray absorption signal.

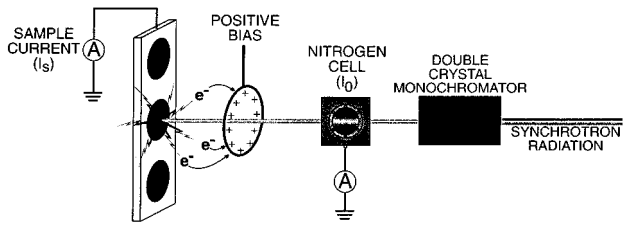

Figure 2. Schematic showing the apparatus used to collect the X-ray absorption signal.

Coin cells using these materials as cathodes and lithium metal foil as the anode were made to test the behavior of these materials upon the electrochemical insertion of lithium. The details of this cell construction have been explained elsewhere.[6] The electrolyte used was 1 M $LiPF_6$ dissolved in a 30/70 volume percent (v/o) mixture of ethylene carbonate and diethyl carbonate. All cells were cycled using a constant current of 18.6 mA/g.

Results

Figure 3 shows the decomposition of the polysiloxane in argon as measured by TGA and RGA. The bottom frame shows the weight (as a percent of the original weight) and dW/dT as a function of temperature. The other frames show the RGA signal for a number of masses. There is no measurable amount of any oxygen-containing gas species in the decomposition stream. Mass 28 could be CO or C_2H_4, but considering that mass 27 shows a virtually identical signal, and that no signal is observed for mass 44 (CO_2), we believe mass 28 is C_2H_4 and mass 27 is C_2H_3.

Figure 4 shows the weight change during HF exposure, as percentage of the initial weight, for each of the nine samples. The samples were removed from HF washing at various times between 1 min and 24 h. Samples 7−9 show no significant change in mass, implying that the reaction has essentially stopped after 8 h and 40% mass loss. Since the HF is in stoichiometric excess to the amount of oxygen present in the sample and that oxygen, by weight, makes up about 40% of the initial Si−O−C, it might initially appear that all the oxygen has been removed, and therefore the reaction has stopped. However, elemental analysis shows that there is a significant amount of oxygen still present. The stoichiometry by elemental analysis is summarized in Table 1. HF will break the Si−O bonds in these materials. However, based on the stoichiometry and weight-loss results, the breaking of these Si−O bonds must be removing not only Si and O but also some C from the material.

(8) Yang, B. X.; Middleton, F. H.; Olssen, B. G.; Bancroft, G. M.; Chen, J. M.; Sham, T. K.; Tan, K.; Wallace, D. J. *Nucl. Instrum. Methods A* **1992**, *316*, 422.

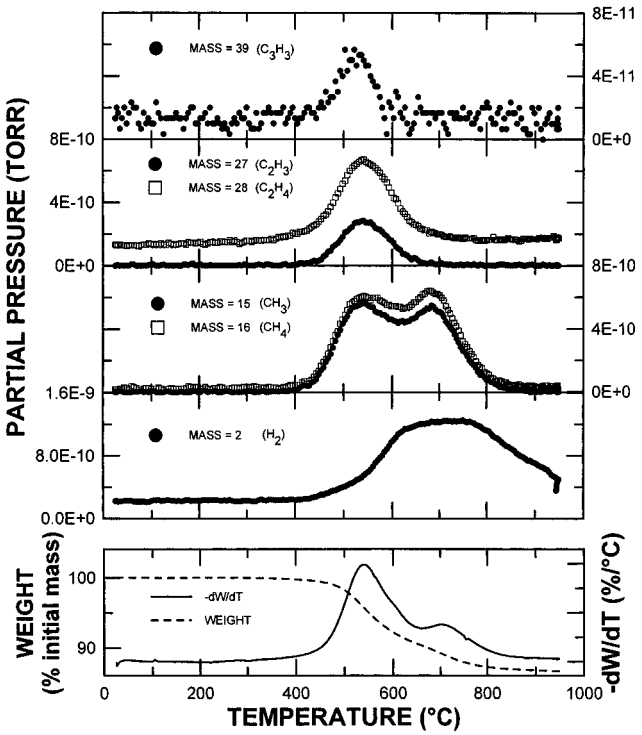

Figure 3. Decomposition of the polysiloxane in argon as a function of temperature; the bottom panel shows the weight as percent of the initial and the derivative of the weight with respect to temperature; the other panels show the RGA signal for various mass numbers.

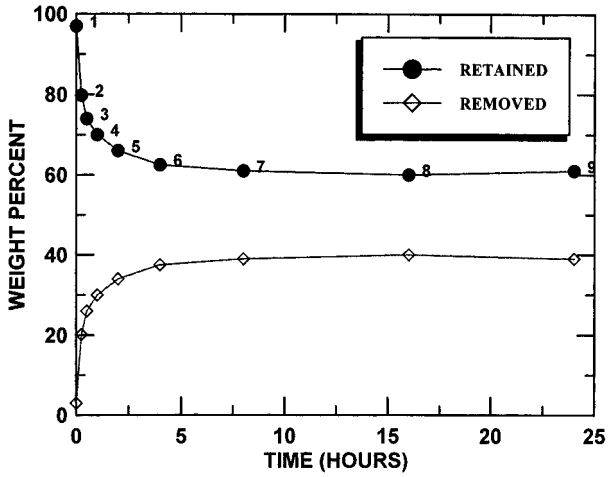

Figure 4. Weight of samples 1−9, plotted as a function of the time when they were removed from the HF solution.

Figure 5 shows the X-ray powder diffraction profiles for samples 1−9. The initial Si−O−C (not HF washed) is indistinguishable from sample 1 and is not shown. Differences in signal-to-noise are due to different counting times and are not dependent on the samples. As we have stated elsewhere,[4,6] we believe these materials consist of a mixture of single graphene sheets and Si−O−C glass. [Graphene sheets are small single-layer fragments of graphite: that is, carbon atoms arranged in the honeycomb arrangement found in graphite. The graphene sheets contain only carbon. The lateral extent of the graphene sheets can be determined from the width of its diffraction peaks, and for the materials discussed here, the graphene sheets average about 25 Å. The Si−O−C glass is thought to have an amorphous structure, similar to SiO_2, with each oxygen involved

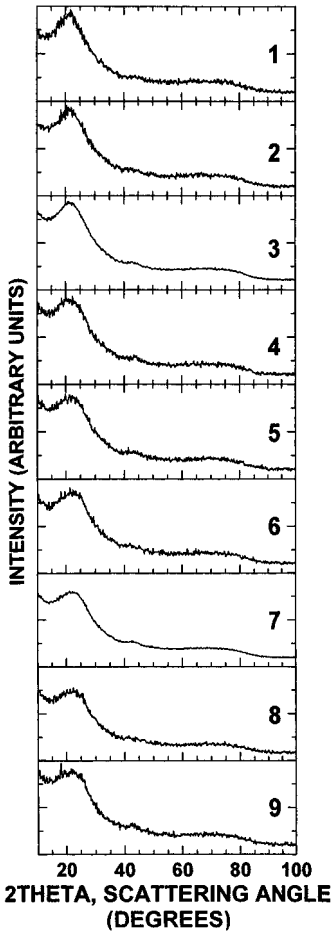

Figure 5. Powder X-ray diffraction profiles for samples 1−9.

Table 1. Summary of the Samples in This Study: Sample 0 Is the Initial Si−O−C Ceramic, before Any Washing in Distilled Water or HF

		wt %			
sample	mass (% of initial)	H	C	Si	O
0	100	0.19	28.7	38.3	26.8
1	97	0.01	21.7	39.8	38.5
2	79.8	0.07	24.8	35.5	39.7
3	74	0.15	27.0	34.3	38.7
4	70	0.01	28.3	35.8	35.9
5	66	0.17	30.1	34.2	35.7
6	62.5	0.11	30.8	34.8	34.4
7	61	0.51	31.2	32.1	38.7
8	60	0.43	31.4	31.6	37.0
9	61	0.55	33.4	33.6	33.1

in two bonds, and each carbon and silicon involved in four bonds. The diffraction pattern of these materials resembles that of amorphous SiO_2. The profiles show features from the Si−O−C network glass centered at 24° and 68°, which are similar to those in a-SiO_2. The peak at 44° arises from the (100) Bragg plane spacing of the graphene sheets.] The change in the profile from sample 1 to 9 is quite small, considering that the material experiences a 40% weight loss. Thus, the bulk structure of the material is virtually unchanged by the HF treatment.

Small-angle scattering of X-rays by powders (SAX) shows regions of differing electron density.[9−11] Regions with characteristic dimensions of 3−100 Å can be

(9) Debye, P.; Anderson, H. R.; Brumberger, H. *J. Appl. Phys.* **1957**, *28*, 679.

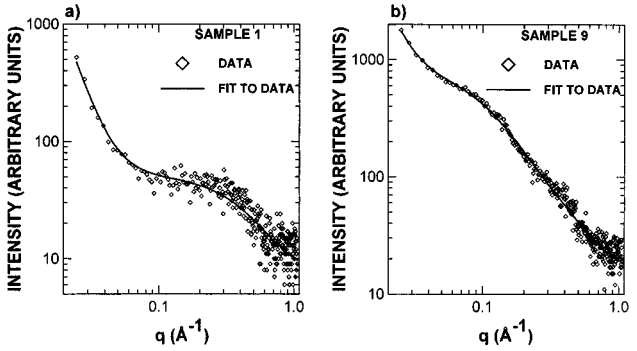

Figure 6. (a) AX data for sample 1 shown with a fit to the data, based on eq 1. (b) SAX data and fit for sample 9.

examined with our diffractometer using Cu Kα radiation. We understand these materials to be a relatively homogeneous network of silicon, oxygen, and carbon atoms mixed with single graphene sheets. Thus, regions of different electron density, of the dimensions we can measure, should correspond to the presence and absence of Si−O−C; that is to say, pores in the powder grains. While the graphene sheets will have different electron densities from the Si−O−C regions, it is believed that these differences are small enough that any contributions from the graphene sheets should be overwhelmed by the presence of pores, which are the complete absence of electrons. [As we will see, the small-angle scattering intensity increases with HF rinsing time, consistent with the creation of more pores and our interpretation.]

The small-angle scattering results were fitted using the form proposed by Debye et al.[9] and extended by Kaliat et al.[10] The intensity, $I(q)$, as a function of the scattered wave vector, q, is taken to be

$$I(q) = \frac{A}{q^n} + \frac{BR_1^4}{(1 + q^2R_1^2)^2} + \frac{CR_2^4}{(1 + q^2R_2^2)^2} + D \quad (1)$$

where R_1 and R_2 are two characteristic correlation lengths for the electron density variations. These can be associated with pore sizes by comparison to Guinier's formula.[11] The radius of gyration of the corresponding pores is $\sqrt{6}$ times R_1 or R_2. A, B, and C are constants proportional to the quantity of macropores, small micropores, and larger micropores, respectively. D represents a constant background. Porod's law[12] for a pinhole scattering system gives $n = 4$. However, in cases where the slits, not pinholes are used, the data are smeared and can give lower apparent values for n in our scattering angle range.[11,13]

To determine n for our system, the sample holder was filled with graphite, a material which contains no micropores. Equation 1 was fit for the graphite data with B and C set to zero, giving $n = 3.55$. For the rest of the fits in this paper, n was set to 3.55.

Figure 6a shows the SAX profile for sample 1 and a fit to these data. Figure 6b shows the SAX profile and fit for sample 9. The fits to the data are close, but they are not ideal. The model used to fit these data is simplified by the use of some assumptions (homogeneous, nonoverlapping pores) which may not be entirely valid for these materials. Still, we believe that the trends observed are well described by the model variables. The corresponding fit variables are summarized in Table 2. The feature centered near 0.1 Å^{-1} corresponds to micropores with a correlation length corresponding to approximately 9 Å. Figure 7 shows the fits (not the original data) to the SAX profile for samples 1−9. Notice that the 0.4 Å^{-1} feature does not appear to change, while the intensity of the 0.1 Å^{-1} feature, absent in sample 1, grows in intensity. An examination of the fit variables shown in Table 2 reveals that the initial micropore distribution, corresponding to a correlation length around $R_1 \approx 2$ Å, undergoes no discernible change in either radius or number density. However, the changes in C and R_2 show clearly that the HF washing introduces micropores with larger correlation lengths, around $R_2 \approx 9.4$ Å. The number of these micropores increases with the duration of HF washing, and the correlation length of the pores decreases to around $R_2 \approx 6.7$ Å.

The BET surface area measurement results are also summarized in Table 2. These results show that the

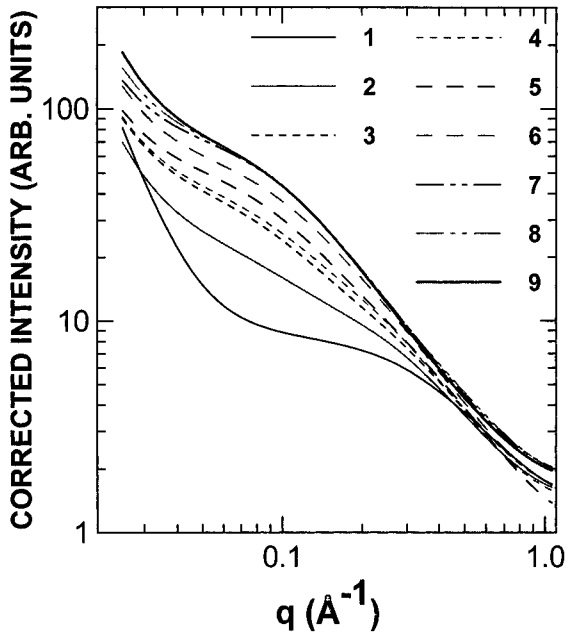

Figure 7. Fits (based on eq 1) to the SAX data for samples 1−9. The formation of additional pores can be seen as the feature at 0.1 Å^{-1} increases in intensity. The data have been corrected for X-ray beam attenuation and mass.

Table 2. Summary of BET Measurements and the Fits to the SAX Data, Based on Eq 2

sample	A	B	R_1	C	R_2	D	surface area (m^2/g)
1	0.0001	0.474	1.76	0	0	0.804	0.25
2	0.0001	0.455	2.18	0.0022	9.35	1.37	17.7
3	0.0001	0.452	2.12	0.0074	8.01	1.23	25.7
4	0.0001	0.371	2.33	0.0070	8.09	1.13	37.1
5	0.0001	0.660	1.93	0.0151	7.34	0.936	44.4
6	0.0001	0.527	2.15	0.0261	6.78	1.44	53.8
7	0.0001	0.481	2.06	0.0291	6.78	1.54	55.6
8	0.0002	0.687	1.91	0.0338	6.78	1.65	54.4
9	0.0002	0.546	2.01	0.0349	6.69	1.67	54.1

(10) Kaliat, M.; Kwak, C. Y.; Schmidt, P. W. *New Approaches in Coal Chemistry*; Blaustein, B. D., Bockrath, B. C., Friedman, S., Eds.; American Chemical Society: Washington DC, 1981; p 3.

(11) Guinier, A.; Fournet, G. (translated by C. B. Walker); *Small-Angle Scattering of X-rays*; John Wiley and Sons: New York, 1955.

(12) Porod, G. Method-General Theory. In *Small Angle X-ray Scattering*; Glatter, O., Kratky, O., Eds.; Academic Press Inc.: London, 1982.

(13) Gibaud, A.; Xue, J. S.; Dahn, J. R. *Carbon* **1996**, *34*, 499.

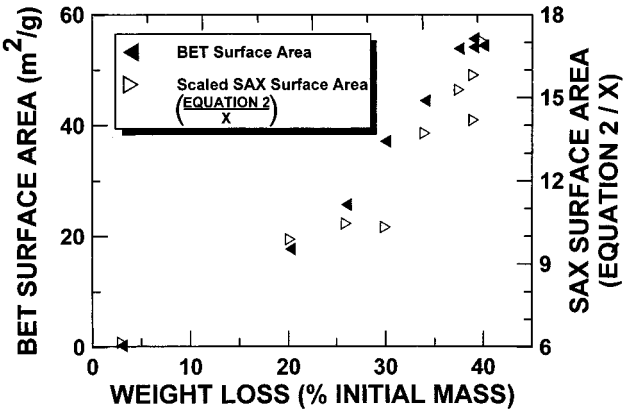

Figure 8. Estimated surface area due to the micropores measured by SAX and the surface area measured by the BET method. Both are plotted versus weight loss due to HF etching.

HF washing results in a continued increase of the surface area with mass loss. To determine whether the surface area results correspond to the fits to the SAX data, a simple approximation is performed. First, it is assumed that all the pores in the material are available to contribute to the surface area. Then the SAX micropore surface area can be estimated, assuming that the pores are spherical, according to

$$SA = 4\,X\pi[BR_1^{\,2} + CR_2^{\,2}] \qquad (2)$$

where SA is the surface area in m^2/g, B, C, R_1, and R_2 are the same as the variables in eq 1, and X is a scaling factor. X includes the conversion from $Å^2$ to m^2, geometrical factors involving the diffractometer, the scattering power of an electron, etc. The results can be used to determine rough agreement between trends observed in the SAX and BET data. The results of applying eq 2 to the fitted variables listed in Table 2 is plotted in Figure 8 along with the BET data. The data presented are eq 2 divided by X and are plotted against the right-hand scale. The nonzero SAX surface area calculated for sample 1 is due to the contributions from the R_1 pores. Both the gas adsorption and small-angle scattering derived surface areas show similar trends with HF etching time. This suggests that all the pores are connected somehow to the sample surface (as expected based on the fact that they were created by an etching reaction) and that micropore formation is entirely responsible for the increase in surface area.

The silicon K-edge X-ray absorption spectra for samples 1, 2, 7, and 9 are shown in Figure 9. For reference purposes c-SiC and c-SiO_2 silicon K-edges were measured and are shown in the bottom panel of Figure 9 (normalized at 1847 eV). The spectra (I_S/I_O) for samples 1, 2, 7, and 9 have been normalized at 1847.4 eV, for comparison of the relative strength of the Si−O bonding to Si−C bonding. Samples 2, 7, and 9 show a feature near 1845.5 eV, attributed to Si−C bonding. This feature increases in relative intensity to the Si−O feature from sample 2 to 9. The stoichiometry change supports this percentage increase in Si−C bonds. It is also believed that this Si−C bonding increase is mainly a surface effect. The measurement has a penetration depth of about 1000 Å or less. Thus, the surface of the material plays a significant role in the absorption signal. If a Si−C passivating region is created on the surface of pore walls, this would result in an increase of the

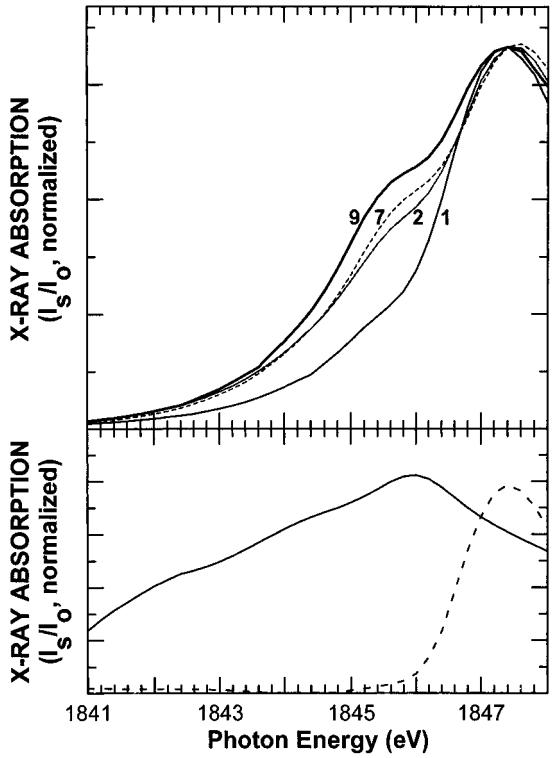

Figure 9. Top panel: Si K-edge for samples 1, 2, 7, and 9 (I_S/I_O normalized at 1847.4 eV). Bottom panel: Si K-edge for SiO_2 (dash) and SiC (solid) (I_S/I_O normalized at 1847 eV).

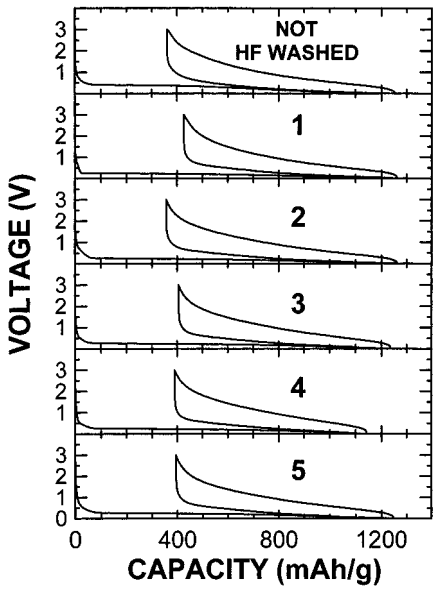

Figure 10. Voltage profiles for cells made from the untreated material and for samples 1−5 as indicated. Note that there is essentially no difference between the profiles for all the samples.

relative Si−C to Si−O signals in the Si K-edge. While the presence of C−C bonding in the material does not contribute to the Si K-edge, it may still be present, in addition to the Si−C bonding.

We have discussed elsewhere[4,6] that the structure of these materials is thought to be a mixture of graphene sheets and Si−O−C network glass. If this is so, then HF washing would remove material only from the Si−O−C regions. The SAX results show that the pores created by the HF washing reach a specific size and do not continue to increase further, implying that the

surface of the pores will not react further with HF under these conditions. We believe that the F^- ions break all the Si−O bonds accessible, until the surface has been etched so that only Si−C and C−C bonds are accessible. Thus, the HF etching reveals or creates a passivating layer. We believe it is this passivating layer which appears in the XAS K-edge data as an increase in Si−C bonding. The decrease in Si and O with respect to C, as shown by elemental analysis, also supports this model.

The intensity of the SAX data and the magnitude of the BET surface areas suggest that these pores must be distributed throughout the bulk of the material. F^- ions are responsible for the formation of the pores and must be able to access the bulk of the material. There must be some larger passages which connect the micropores formed by HF etching. This is likely why eq 1 was not sufficient to achieve a better fit to the SAX data. It assumes that the pores are noninteracting which is probably not the case.

Figure 10 summarizes the electrochemical measurements made on these materials. The first discharge and charge and second discharge are shown for a cell of materials 1−5. Included for comparison are data from Si−O−C material before any washing in water or in HF. The slight differences between cells is within our error range and should not be attributed to differences between the materials.

Conclusions

The HF washing of a Si−O−C glass introduces micropores into the bulk of the material, resulting in up to a 40% mass loss. Despite the presence of more than enough HF to react with all the oxygen in the material, there is little change in the ratio of silicon to oxygen, although the fractions of silicon and oxygen decrease with respect to the fraction of carbon present. The lack of continued mass loss with time and the Si K-edge data suggests that a silicon−carbon passivation surface is created or revealed by etching. We believe that it is this passivation surface that prevents the further HF etching of the material.

Despite the change in surface chemistry, pore morphology and the slight change in stoichiometry, the voltage profile of these materials upon insertion of lithium did not change. Thus it is the bulk, and not the surface, of these Si−O−C materials which is involved in reversible and irreversible lithium reactions. Our initial hope of a method to change the stoichiometry of the glasses at room temperature, and their electrochemical properties, was not realized.

Acknowledgment. We wish to acknowledge Moli Energy (1990) Ltd. for the use of equipment to perform the BET surface area measurements.

CM970224P